BIOCHEMISTRY
including biophysical chemistry & molecular biology
Article

Biochemistry **2009,** *48,* 10113–10119 10113
DOI: 10.1021/bi9012275

Effect of a Domain-Spanning Disulfide on Aminoacyl-tRNA Synthetase Activity†

Papri Banerjee, M. Bryan Warf,‡ and Rebecca Alexander*

Department of Chemistry, Wake Forest University, Winston-Salem, North Carolina 27109. ‡*Current address: Institute of Molecular Biology, University of Oregon, Eugene, OR 97403.*

Received July 18, 2009; Revised Manuscript Received August 28, 2009

ABSTRACT: Enzymes regulated by allostery undergo conformational rearrangement upon binding effector molecules. For modular proteins, a flexible interface may mediate reorientation of the protein domains and transmit binding events to activate catalysis at a distance. Aminoacyl-tRNA synthetases (aaRSs) that use tRNA anticodons as identity elements can be considered allosteric enzymes in which aminoacylation of the tRNA acceptor stem is enhanced upon anticodon binding. We reasoned that anticodon-triggered conformational change might be restricted upon introduction of a disulfide linkage near the core of an aaRS. Here we show that a double cysteine mutation engineered at the *Escherichia coli* MetRS domain interface spontaneously generates a disulfide linkage. This disulfide clamp has no effect on methionyl adenylate formation but reduces the level of $tRNA^{Met}$ aminoacylation ~2-fold. Activity is restored upon chemical reduction of the disulfide, demonstrating that *E. coli* MetRS requires a flexible interface domain for full catalytic efficiency.

Proteins are dynamic macromolecules that undergo structural rearrangement to bind ligand, regulate access to a catalytic site, or release product. Conformational flexibility is essential for Koshland's classical "induced fit" model of enzyme regulation, in which ligand binding alters protein structure to promote catalysis (*1*). Despite numerous high-resolution structures that sample a protein's conformational landscape upon ligand binding, the energetic contribution of protein flexibility to catalysis is poorly understood. Furthermore, the physical and energetic paths of long-range communication are characterized for few enzymes. Here we report the contribution of conformational flexibility to catalytic activation in an aminoacyl-tRNA synthetase.

Aminoacyl-tRNA synthetases (aaRSs) catalyze the attachment of amino acids to their cognate tRNAs, thereby establishing the rules of the genetic code (*2*). Synthetases are modular proteins, with distinct polypeptide elements contributing catalytic, tRNA binding, and editing functions. Biochemical and structural analyses reveal that tRNA aminoacylation has features of allosteric catalysis, such that binding of an effector (for example, the tRNA anticodon) results in a change in shape from an inactive to active enzyme. It is particularly clear that for enzymes using nucleotide determinants outside the acceptor arm, communication between protein domains contributes to efficient tRNA aminoacylation (*3*). aaRS conformational changes observed or predicted upon tRNA binding include rearrangement of surface loops (*4*), rotation of domains relative to one another (*5*−*7*), hinge-bending reorientation of domains (*8*, *9*), and assembly of the catalytic domain (*10*, *11*).

Methionyl-tRNA synthetase (MetRS) has a strong dependence on the CAU anticodon of its isoaccepting tRNAs, such that anticodon substitutions decrease aminoacylation efficiency (k_{cat}/K_M) as much as 6 orders of magnitude (*12*). Because anticodon nucleotides are critical for $tRNA^{Met}$ aminoacylation, small RNA substrates that recapitulate the tRNA acceptor stem but lack the anticodon are poor substrates for MetRS (*13*, *14*). The C-terminal anticodon binding domain of *Escherichia coli* MetRS (Figure 1) is an α-helical bundle containing Trp-461, which contacts the CAU anticodon and is essential for cognate tRNA selection (*15*, *16*). The extreme C-terminal portion of MetRS contains a dimerization domain that is dispensable for activity in vitro (*17*). The crystal structure of the *Aquifex aeolicus* MetRS−$tRNA^{Met}$ complex demonstrated that Trp-422 (which aligns with *E. coli* Trp-461) stacks on C34 (*7*). While the extreme 3′-terminus of $tRNA^{Met}$ was disordered in the crystal structure, biochemical evidence (*18*) suggests that cognate anticodon binding triggers unwinding of the tRNA acceptor stem to produce the acceptor stem hairpin observed for tRNAs aminoacylated by class I ArgRS, CysRS, GlnRS, GluRS, and LeuRS (*10*, *19*−*22*).

The N-terminal catalytic domain of *E. coli* MetRS synthesizes methionyl adenylate and aminoacylates small RNA substrates even with an anticodon binding domain rendered inactive by mutations (*23*). Likewise, the anticodon binding domain retains nucleotide discrimination despite mutations that diminish tRNA aminoacylation activity (*24*). It is clear that for MetRS, efficient aminoacylation requires functional communication between these protein modules, and that conformational change is a likely mechanism for interdomain communication (*25*−*27*). We hypothesized that if anticodon-triggered conformational change is important for efficient $tRNA^{Met}$ aminoacylation, mutations that limit the flexibility of MetRS should inhibit catalysis.

Introduction of non-native disulfide bonds within proteins thought to undergo conformational change has proven to be informative for a variety of systems, including RNA polymerase (*28*−*31*), *E. coli* 5′-nucleotidase (*32*), and a cold-adapted alkaline phosphatase (*33*). We sought to use an engineered

†This work was supported by Grant MCB-0448243 from the National Science Foundation and by the National Foundation for Cancer Research.

*To whom correspondence should be addressed. E-mail: alexanr@wfu.edu. Phone: (336) 758-5568. Fax: (336) 758-4656.

Published on Web 09/22/2009

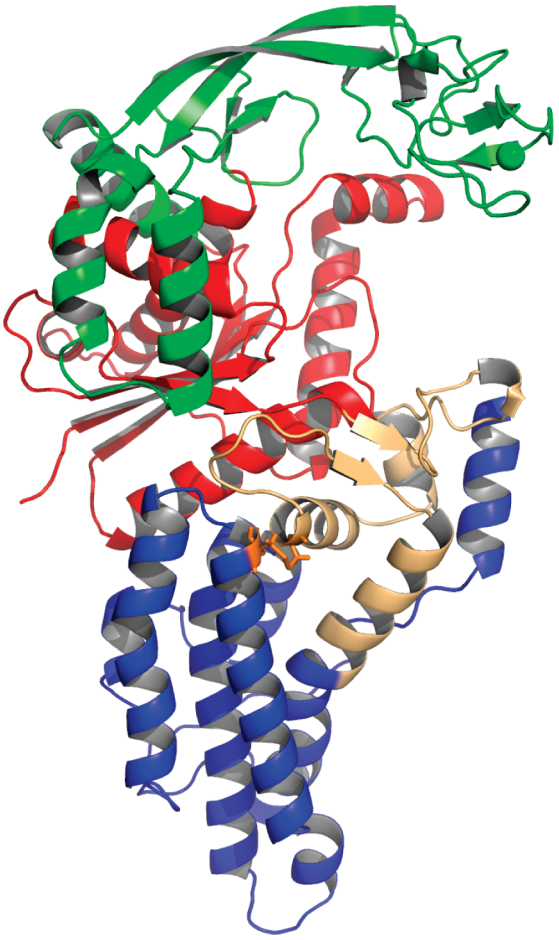

FIGURE 1: *E. coli* MetRS showing the locations of cysteine mutants generated. Monomeric *E. coli* MetRS [Protein Data Bank (PDB) entry 1QQT] is shown with the Rossmann nucleotide binding domain (active site) colored red, the connective polypeptide green, the stem contact fold gold, and the anticodon binding domain blue. Substitutions to cysteine are colored orange at residues 361 (stem contact fold) and 438 (anticodon binding domain).

disulfide linkage to probe the conformational flexibility of the interdomain region of MetRS and determine the contribution of flexibility to $tRNA^{Met}$ aminoacylation efficiency.

MetRS contains a helical subdomain between its anticodon and catalytic domains that includes a helix−turn−strand−helix motif also observed for GlnRS (*34*) and other class I aaRSs. In the GlnRS−$tRNA^{Gln}$ complex, the loop of this motif is directed at the inner corner of $tRNA^{Gln}$, likely mediating the proper orientation of $tRNA^{Gln}$ into the enzyme's active site (*19*). Modeling analysis predicted a similar orientation for the MetRS−:$tRNA^{Met}$ complex (*34*), and we reasoned that the structurally similar peptide at MetRS's interface might serve a functional role in the induced fit mechanism of cognate tRNA selection. Guided by the *E. coli* MetRS crystal structure (PDB entry 1QQT), we identified four pairs of amino acids that span the stem contact fold and the anticodon binding or catalytic domain with a Cα separation of < 7 Å. We show that substitution of Ala-361 and Gly-438 with cysteine residues results in spontaneous formation of a non-native disulfide bond that reversibly inhibits anticodon-triggered $tRNA^{Met}$ aminoacylation ~2-fold without altering methionyl adenylate formation.

MATERIALS AND METHODS

Cloning and Purification of E. coli Methionyl-tRNA Synthetase Variants. The portion of the *metS* gene corresponding to the 547 N-terminal amino acids of *E. coli* MetRS was cloned into pET28a (Novagen, Gibbstown, NJ) to generate pSW101, which encodes an N-terminally His_6-tagged MetRS monomer. A similar His_6-MetRS monomer was previously shown to be fully active in functional assays (*18*). Pairs of residues chosen for disulfide engineering were Ile-367 and His-323, Asp-368 and Gly-324, Asn-329 and Asn-373, and Ala-361 and Gly-438. Single-cysteine substitutions at each position and the double mutants Asn-329 → Cys/Asn-373 → Cys and Ala-361 → Cys/Gly-438 → Cys were generated by QuikChange mutagenesis (Stratagene, La Jolla, CA) of pSW101. The presence of mutations was confirmed by DNA sequencing. Wild-type and mutant proteins were purified to homogeneity from Rosetta 2 (DE3) cells (Novagen) by nickel affinity chromatography according to the manufacturer's protocol (Qiagen, Valencia, CA). Purified MetRS variants were flash-frozen and stored in 20 mM HEPES-KOH (pH 7.5), 100 mM NaCl, 10 mM KCl, 10 mM $MgCl_2$, and 40% glycerol at −80 °C and used directly for assays. Protein concentrations were measured by a microplate Bradford assay (Bio-Rad) using BSA as the standard.

Liquid Chromatography−Mass Spectrometry (LC−MS) Identification of Disulfide. Mass spectrometry analysis was conducted at the Protein Analysis Core Laboratory of the Cleveland Clinic Research Foundation (Cleveland, OH). Purified wild-type MetRS and the G438C/A361C variant were electrophoresed on a 10% sodium dodecyl sulfate−polyacrylamide gel electrophoresis (SDS−PAGE) gel and stained with Coomassie blue. Protein bands were cut into small pieces, washed with water, and dehydrated in acetonitrile. Samples were alkylated with iodoacetamide before in-gel trypsin digest. The peptides were extracted from the polyacrylamide in two aliquots of 30 μL of 50% acetonitrile with 5% formic acid. These extracts were combined and evaporated to < 10 μL and then resuspended in 1% acetic acid, yielding a final volume of ~30 μL for LC−MS analysis. The LC−MS system is a Finnigan LTQ linear ion trap mass spectrometer interfaced with an Eksigent splitless nanoflow HPLC system [self-packed 9 cm × 75 μm (inside diameter) Phenomenex Jupiter C18 reversed-phase capillary chromatography column]. The peptides from 10 μL of tryptic digest eluted from the column by an acetonitrile/0.05 M acetic acid gradient at a flow rate of 200 nL/min were introduced directly into the microelectrospray ion source (2.5 kV) of the mass spectrometer. The digest was analyzed, and peptides were identified by full scanning of the mass spectra. Peptide coverage was 76% for wild-type MetRS and 77% for the A361C/G438C variant (51 peptides each). Further confirmation of peptide identity was achieved by collision-induced dissociation (CID).

Quantification of Reactive Thiols. The number of free sulfhydryl groups present in MetRS variants was determined using DTNB [5,5′-dithiobis(2-nitrobenzoic acid)], Ellman's reagent (Pierce/ThermoScientific, Rockford, IL), which undergoes disulfide exchange with protein thiols to release 2-nitro-5-thiobenzoate (NTB) ($\lambda_{max} = 412$ nm; $\varepsilon_{412} = 14150\ M^{-1}\ cm^{-1}$) (*35*). MetRS (18 μM) was incubated at room temperature for 15 min with 0.18 mM DTNB in 0.1 M sodium phosphate (pH 8.0), 1 mM EDTA, and 8 M urea. The concentration of reactive thiols present in each sample was calculated from NTB absorbance at 412 nm using Beer's law. Determinations were performed in triplicate.

Reduction of the Disulfide Bond. The engineered disulfide in the A361C/G438C variant was reduced by incubation at 25 °C for 45−60 min with tris(2-carboxyethyl)phosphine hydrochloride

(TCEP-HCl) agarose (Pierce/ThermoScientific) according to the manufacturer's protocol. Following removal of the reductant using a spin column, reduced protein was used within 30 min for either thiol quantification or tRNA aminoacylation.

Preparation of RNA Substrates. $tRNA^{Met}$ was generated by in vitro transcription of overlapping oligonucleotides (*36*) using T7 RNA polymerase, NTPs (5 mM each), 40 mM DTT, 250 mM HEPES-KOH (pH 7.5), 30 mM $MgCl_2$, and 0.1 mg/mL bovine serum albumin at 37 °C for 2 h. Transcription products were purified on 16% denaturing polyacrylamide gels and electroeluted using an Elutrap device (Schleicher & Schuell, Keene, NH). The concentration of $tRNA^{Met}$ was determined by the absorption at A_{260} (1 OD unit = 40 mg/L; $tRNA^{Met}$ molecular mass of 23480 Da), and the chargeability was determined by a plateau charging assay. Purified tRNA was typically aminoacylated at >80% of the A_{260}-determined RNA concentration.

Methionyl Adenylate Assay. Enzyme-catalyzed formation of methionyl adenylate was monitored in a $^{32}PP_i$−ATP exchange assay as described previously (*24*). The reaction mixture contained 100 mM Tris-HCl (pH 7.5), 2 mM $NaPP_i$, 10 mM 2-mercaptoethanol, 0.1 mg/mL BSA, 10 mM KF, 5 mM $MgCl_2$, 2 mM ATP, 20 μM methionine, and [^{32}P]$NaPP_i$ (1−60 Ci/mmol). Reactions were performed at 25 °C and initiated by addition of enzyme (final concentration of 50 nM). Aliquots (10 μL) were removed at 2 min intervals and reactions quenched with 500 μL of charcoal suspension (3% charcoal in 7% $HClO_4$ and 0.2 M PP_i). The quenched reaction mixture was spun twice at 16000 rpm with 0.2 mL of wash buffer (10 mM PP_i and 0.5% $HClO_4$). The [γ-^{32}P]ATP generated by the exchange reaction and trapped in the charcoal was collected in a spin column and quantified by scintillation counting.

Aminoacylation of tRNA. tRNA aminoacylation assays were conducted as described previously (*24*). We annealed samples by heating them to 80 °C in 20 mM HEPES-KOH (pH 7.5), slowly cooling them to 60 °C, adding $MgCl_2$ to a final concentration of 1 mM, and then cooling them to room temperature. Annealed tRNA (1−100 μM) was incubated with MetRS (50 nM) in 150 mM NH_4Cl, 20 mM HEPES-KOH (pH 7.5), 10 mM $MgCl_2$, 4 mM ATP, 0.1 mM EDTA, 100 μM methionine, and [^{35}S]methionine (>1000 Ci/mmol). Assays to determine kinetic parameters of tRNA aminoacylation were performed at least in duplicate with 50 nM wild type and tRNA concentrations ranging from 2 to 20 μM $tRNA^{Met}$. Kinetic parameters were generated from hyperbolic fits of the initial velocity of tRNA aminoacylation versus $tRNA^{Met}$ concentration using Origin 8.0 (OriginLab Corp., Northampton, MA).

RESULTS

Preparation of MetRS Variants. Single-cysteine variants of His_6-MetRS at His-323, Gly-324, Asn-329, Ala-361, Ile-367, Asp-368, Asn-373, and Gly-438 were prepared by QuikChange mutagenesis of the pET28-cloned MetRS monomer (pSW101) and verified by DNA sequencing. Proteins were soluble on expression in Rosetta 2 (DE3) cells and were purified by nickel affinity chromatography to homogeneity. Activity assays revealed that His-323 and Gly-324 were sufficiently impaired in activity that double-cysteine variants including these residues were not constructed. Double mutants Asn-329 → Cys/Asn-373 → Cys (N329C/N373C) and Ala-361 → Cys/Gly-438 → Cys (A361C/G438C) were generated by the QuikChange method. The N329C/N373C variant was insoluble under growth conditions used and was not pursued. The A361C/G438C double-cysteine variant, verified by sequencing the entire gene, was solubly expressed in Rosetta 2 (DE3) cells.

Presence of a Disulfide Bond. It was not clear from the outset whether merely introducing proximal cysteine residues into the MetRS sequence would generate a disulfide bond or whether external oxidants or cross-linking agents would be necessary. The presence of a spontaneously formed disulfide bond in affinity-purified A361C/G438C MetRS was suggested by the reaction of MetRS variants with DTNB. The native *E. coli* MetRS monomer (547 N-terminal residues) has eight cysteine residues and no disulfide bonds (*15*). Four of these cysteines chelate a Zn^{2+} in the connective polypeptide motif inserted between halves of the Rossmann fold domain (*37*, *38*) and are not reactive to DTNB even under moderate denaturing conditions (8 M urea). Thus, only 4 equiv of thiolate ion is produced upon treatment of wild-type MetRS with DTNB under denaturing conditions (Figure 2). Incubation with DTNB revealed five reactive thiols for the Gly-438 → Cys mutant but only four for the A361C/G438C double mutant. This spectroscopic analysis suggested the presence of a spontaneously formed disulfide bond in the A361C/G438C variant. The disulfide could be reduced by treatment with agarose-immobilized TCEP, resulting in six thiols per protein detected upon reaction with DTNB (Figure 2). Reduced protein reoxidized within 30 min at ambient temperature, indicating that the engineered cysteine thiols were ideally oriented for disulfide formation.

To determine whether the disulfide was formed between the engineered cysteine side chains, mass spectrometric analysis was conducted. Trypsin digestion of the A361C/G438C variant followed by LC−MS revealed mass peaks at $[M + 2H]^{2+} - H_2O$ (673.25 Da) and $[M + 3H]^{3+} - H_2O$ (449.06 Da) corresponding to the disulfide-linked peptide ^{357}YYYTCK^{362}-^{436}EFCK^{439} (1365 Da) (Figure 1 of the Supporting Information). This peptide was not detected in wild-type MetRS. Given the rate of reoxidation of the disulfide, mass spectroscopy analysis of the reduced protein was not pursued.

Methionyl Adenylate Formation. Ala-361 and Gly-438 are remote from MetRS's active site, with their α-carbons 25.2 and 26.0 Å, respectively, from the carbon representing the reactive carbonyl in the methionyl adenylate analogue of PDB entry 1PG0 (*39*). To determine whether substitution of either residue with cysteine would affect catalysis in the active site, we monitored methionyl adenylate formation using a ^{32}P isotope exchange assay (*40*). As expected, methionyl adenylate formation was unaffected by the disulfide bond formed in the A361C/G438C variant (Figure 3).

$tRNA^{Met}$ Aminoacylation. In vitro-transcribed initiator $tRNA^{Met}$ was used as a substrate for MetRS variants in the standard trichloroacetic acid precipitation assay under multiple-turnover conditions (50 nM enzyme and 2 μM tRNA). Substitution of either Ala-361 or Gly-438 with cysteine had no effect on tRNA aminoacylation, while the A361C/G438C disulfide-containing variant demonstrated a modest reduction in activity (Figure 4). Kinetic analysis of the wild-type and A361C/G438C enzymes indicated that k_{cat} decreases ~2-fold, while K_M values are not statistically different (Table 1). While modest, the decrease in the level of tRNA aminoacylation can be attributed to the presence of the engineered disulfide. Treatment of A361C/G438C MetRS with TCEP reductant immediately prior to the aminoacylation assay resulted in full recovery of activity without affecting wild-type MetRS activity (Figure 5).

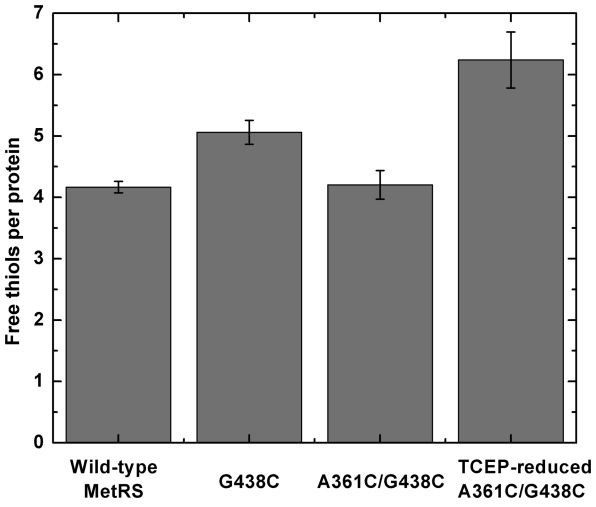

FIGURE 2: Quantitation of reactive thiols using Ellman's reagent. MetRS variants were reacted with 5,5′-dithiobis(2-nitrobenzoic acid) (DTNB, Ellman's reagent) under denaturing conditions to determine the number of solvent-accessible thiol groups. Error bars indicate standard deviations from three determinations.

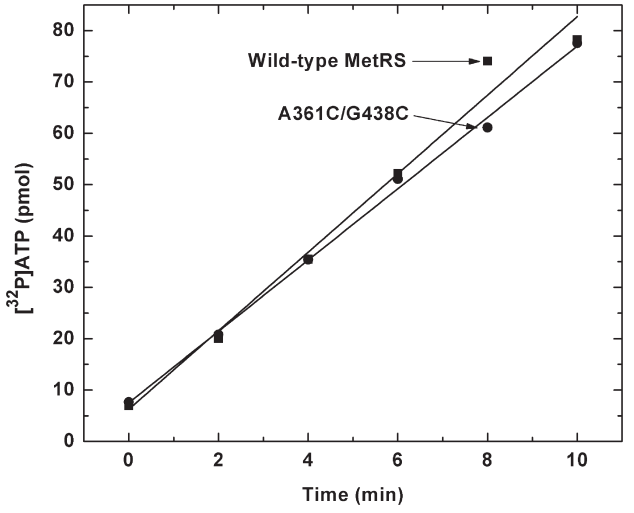

FIGURE 3: Methionyl adenylate formation by MetRS variants. Wild-type or A361C/G438C MetRS (50 nM each) was assayed for methionyl adenylate activity by monitoring enzyme-dependent incorporation of the ^{32}P label from radiolabeled inorganic pyrophosphate into ATP.

DISCUSSION

The functional polypeptide modules of aaRSs adopt a variety of conformations depending on the presence of tRNA or small molecule substrates and the catalytic state of the enzyme. For example, the connective polypeptide (CP) domain of *Thermus thermophilus* leucyl-tRNA synthetase (LeuRS), responsible for hydrolytic editing of misaminoacylated tRNA^{Leu}, rotates 35° away from the LeuRS core upon forming an editing complex (*41*). Flexibility of this hinge is necessary for the editing activity of LeuRS (*42*). The short β-strand linkers connecting the CP domains of several class I aaRSs are hinge points for conformational reorientation, as demonstrated biochemically (*42*) and computationally (*25*, *43*). The C-terminal domains of some aaRSs, such as CysRS (*21*) and TyrRS (*44*), are also attached by flexible linkers. Similarly, flexibility of the class I-defining KMSKS surface loop is critical for aminoacyl adenylate formation, as demonstrated for MetRS via replacement of glycine residues at the ends of the KMSKS loop with proline residues (*45*).

A crystal structure of *E. coli* MetRS complexed with its cognate tRNA^{Met} remains elusive, although the 2.7 Å structure of the corresponding *A. aeolicus* complex allows predictions to be made concerning the conformational changes likely to occur upon cognate tRNA binding. (*A. aeolicus* and *E. coli* MetRS

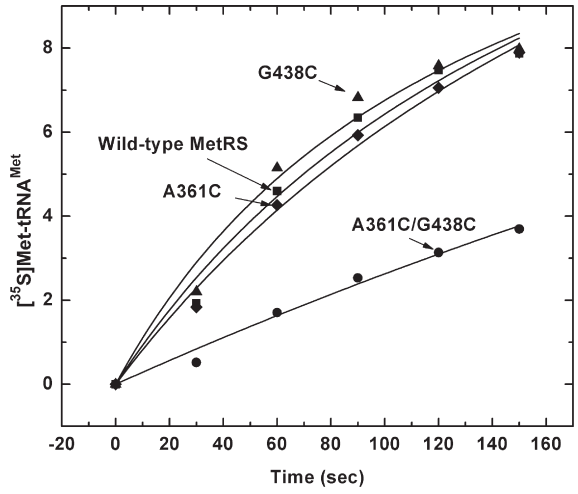

FIGURE 4: tRNA^{Met} aminoacylation by MetRS variants. tRNA^{Met} (2 μM) was incubated at 25 °C with 50 nM wild-type MetRS, single variant Ala-361 → Cys or Gly-438 → Cys, or the disulfide-containing A361C/G438C variant.

Table 1: Steady-State Kinetic Parameters for tRNA^{Met} Aminoacylation[a]

enzyme	K_M (μM)	k_{cat} (s^{-1})
wild-type MetRS	4.6 ± 1.7	0.92 ± 0.25
G438C/A361C	6.1 ± 2.0	0.46 ± 0.10

[a]Enzymes were assayed at 50 nM, with saturating concentrations of ATP and methionine. The tRNA^{Met} concentration was varied from 0.2 to 20 μM. Kinetic parameters were determined by nonlinear curve fitting using Origin 8.0 (OriginLab Corp.). Errors in K_M and k_{cat} are standard deviations of five measurements.

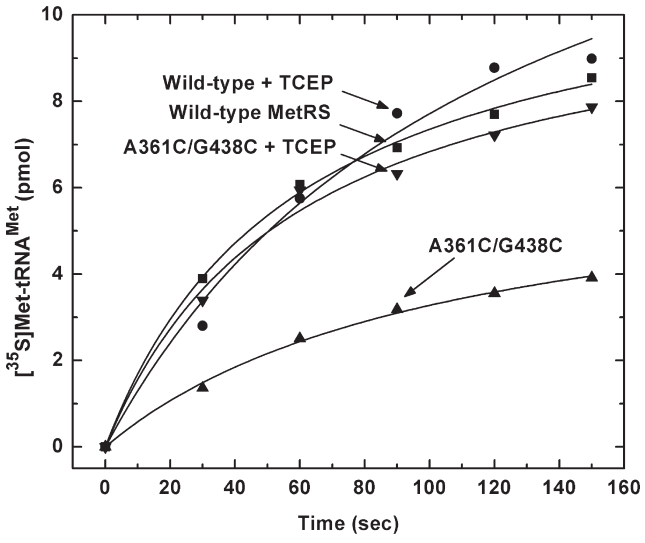

FIGURE 5: Recovery of catalytic activity upon disulfide reduction. tRNA^{Met} (2 μM) was incubated at 25 °C with 50 nM wild-type MetRS or A361C/G438C variant. Proteins were used as purified (nonreducing conditions) or following treatment with agarose-immobilized TCEP.

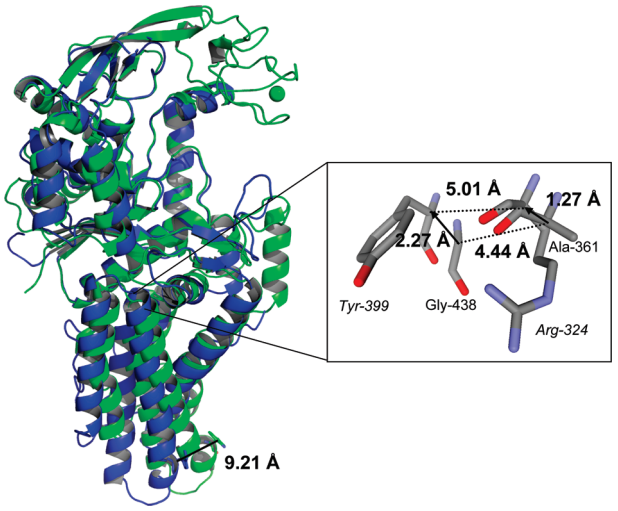

FIGURE 6: Inferred MetRS conformational changes upon tRNA binding. *E. coli* MetRS [PDB entry 1QQT (green)] is superimposed with *A. aeolicus* $tRNA^{Met}$-bound MetRS [PDB entry 2CSX (blue)] using the MultiProt alignment server. In the inset, residues Ala-361 and Gly-438 of *E. coli* MetRS are shown with the corresponding AaMRS Arg-324 and Tyr-399 residues (in italics) of *A. aeolicus* MetRS. For the sake of clarity, the inset figure is rotated −75° around the protein's long axis relative to the full protein structure shown at the right. Distances shown are between Cα atoms.

exhibit 25% identical and 43% similar amino acids, excluding the C-terminal dimerization domain idiosyncratic to *E. coli* MetRS.) In the *A. aeolicus* structure, the MetRS CP domain and tRNA 3′-end are disordered, suggesting high mobility in these regions. High mobility of the CP domain was also observed in all-atom, explicit solvent molecular dynamics simulations of ligand-free *E. coli* MetRS (*25*). It remains to be seen whether the CP domain of MetRS, variable in length and zinc content among MetRS phylogenetic clusters (*15*), rearranges in a defined way upon $tRNA^{Met}$ binding. Comparison of the (*A. aeolicus*) tRNA-bound protein with its (*E. coli*) apo form suggests that the C-terminal anticodon binding domain rotates approximately 15° relative to the protein's catalytic core upon tRNA binding (*7*). Molecular dynamics simulations indicated that the rotated conformation is accessible even without tRNA, suggesting inherent deformability of the protein at the domain interface (*25*).

Given that the catalytic and anticodon binding domains of MetRS likely undergo a rigid body rotation that is stabilized by tRNA binding (rather than a hinge-bending reorientation as seen or predicted for tethered CP and C-terminal domains of other aaRSs), it was not clear whether introduction of a disulfide at the core of the enzyme would have any impact on catalysis. If the two major domains rotate relative to one another, the domain interface where cysteine residues were introduced can be considered the pivot point and undergo only minimal displacement upon domain rotation. Alignment of the active sites of *A. aeolicus* MetRS (from PDB entry 2CSX) and *E. coli* MetRS (from PDB entry 1QQT) produces a root-mean-square deviation of 1.29 Å over 242 N-terminal residues [MultiProt alignment server (http://bioinfo3d.cs.tau.ac.il/MultiProt/)]. The residues of *A. aeolicus* MetRS in positional correspondence with Ala-361 and Gly-438 of *E. coli* MetRS are Arg-324 and Thr-399, respectively. With the active sites of each protein aligned, Ala-361 and Gly-438 are 4.44 Å apart in 1QQT, and the corresponding residues are 5.01 Å apart in 2CSX (Figure 6, in which all distances refer to Cα positions). The absolute change in position of these residues, representing the rotation of the anticodon binding domain relative to the active site domain, is somewhat greater. With active sites aligned, Arg-324 moves 1.27 Å from Ala-361 and Tyr-399 moves 2.27 Å from Gly-438. The greatest absolute positional change observed upon tRNA binding occurs at the distal end of the protein's helical bundle domain. The highly conserved tryptophan residue that mediates C34 recognition (Trp-461 in *E. coli* and Trp-422 in *A. aeolicus*) moves 9.21 Å (Figure 6).

Given the limited degree of conformational change in *E. coli* MetRS predicted to occur upon $tRNA^{Met}$ binding in light of the *Aquifex* complex structure (*7*), it is perhaps surprising that even a modest, reversible reduction in the level of tRNA aminoacylation is observed upon introduction of an interdomain disulfide bond. The negligible distance change between the corresponding residues of *A. aeolicus* MetRS would not be precluded by the presence of a disulfide, as the distance threshold for disulfide cysteine Cα atoms is 7 Å (*46*). Furthermore, disulfide bonds limit but do not prevent protein mobility. In other enzymes where the quantitative effects of disulfide bond formation have been measured, a wide range of activity decreases are reported depending on the magnitude of conformational change in the native catalytic system. For example, the periplasmic *E. coli* 5′-nucleotidase is predicted to undergo a dramatic domain rotation (up to 96°) to bring the catalytic and substrate sites into the proximity of one another for phosphate ester hydrolysis (*32*). Engineering a disulfide that locks the enzyme into a conformation intermediate between its inactive (open) and active (closed) states results in 2-fold reduction in k_{cat} for catalysis (with no effect on K_M), while a separate disulfide that locks the enzyme open results in complete inactivation of the enzyme (*32*). For a cold-adapted *Vibrio* sp. alkaline phosphatase, introduction of disulfide bonds reduces k_{cat} 6−16-fold (*33*). Thus, the 2-fold decrease in k_{cat} for the disulfide-containing A361C/G438C MetRS variant is consistent with the magnitude of motion likely to occur at the core of MetRS. The conformational rearrangement of anticodon binding and catalytic domains impaired here by an engineered disulfide represents only a small component of anticodon-triggered aminoacylation of the tRNA acceptor stem. In contrast, removal of the anticodon−MetRS interaction through a Trp-461 → Ala substitution (*47*) or use of small RNA substrates lacking the anticodon (*13*, *14*) results in a dramatic 10^5-fold decrease in catalytic activity. It should be noted that RNA binding is impaired for both the microhelix substrate and the Trp-461 substitution, while introduction of the interdomain disulfide affects only k_{cat} of the tRNA aminoacylation reaction, not K_M (Table 1).

In the absence of a $tRNA^{Met}$−MetRS cocrystal structure that would reveal interactions between the tRNA acceptor stem and CP domain, it is difficult to predict where a single disulfide clamp would elicit a more dramatic effect on tRNA aminoacylation, either by reversibly diminishing activity to a greater degree than shown here or by enhancing activity by locking the protein in a "tRNA-bound" conformation. Other than the zinc-binding CP domain, there are not appended protein modules connected by a flexible tether as with other aaRSs such as the leucine-specific domain of *T. thermophilus* LeuRS (*41*), the extreme C-terminal anticodon-binding domain of CysRS (*21*), the N-terminal tRNA binding domain of *Methanosarcina barkeri* SerRS (*48*), or the C-terminal tRNA binding domain of human mitochondrial PheRS (*9*). It is likely that the catalytic activity of one or more other aaRSs may be more severely impaired upon

introduction of an engineered disulfide than what is seen here for MetRS.

ACKNOWLEDGMENT

We thank Paul Schimmel for valuable discussions and comments on an early version of the manuscript and Michael Budiman for advice on LC−MS.

SUPPORTING INFORMATION AVAILABLE

One figure showing mass spectroscopic analysis of trypsin-digested A361C/G438C MetRS. This material is available free of charge via the Internet at http://pubs.acs.org.

NOTE ADDED IN PROOF

A disulfide bond engineered at the interface of functional domains in human mitochondrial PheRS has recently been demonstrated to impair amino acid transfer to tRNA without affecting adenylate formation, as shown here for *E. coli* MetRS (*49*).

REFERENCES

1. Koshland, D. E.Jr. (1958) Application of a theory of enzyme specificity to protein synthesis. *Proc. Natl. Acad. Sci. U.S.A. 44*, 98–104.
2. Ibba, M., and Soll, D. (2000) Aminoacyl-tRNA synthesis. *Annu. Rev. Biochem. 69*, 617–650.
3. Alexander, R. W., and Schimmel, P. (2001) Domain-domain communication in aminoacyl-tRNA synthetases. *Prog. Nucleic Acid Res. Mol. Biol. 69*, 317–349.
4. Yaremchuk, A., Tukalo, M., Grotli, M., and Cusack, S. (2001) A succession of substrate induced conformational changes ensures the amino acid specificity of *Thermus thermophilus* prolyl-tRNA synthetase: Comparison with histidyl-tRNA synthetase. *J. Mol. Biol. 309*, 989–1002.
5. Silvian, L. F., Wang, J., and Steitz, T. A. (1999) Insights into editing from an Ile-tRNA synthetase structure with $tRNA^{Ile}$ and mupirocin. *Science 285*, 1074–1077.
6. Sauter, C., Lorber, B., Cavarelli, J., Moras, D., and Giege, R. (2000) The free yeast aspartyl-tRNA synthetase differs from the tRNA(Asp)-complexed enzyme by structural changes in the catalytic site, hinge region, and anticodon-binding domain. *J. Mol. Biol. 299*, 1313–1324.
7. Nakanishi, K., Ogiso, Y., Nakama, T., Fukai, S., and Nureki, O. (2005) Structural basis for anticodon recognition by methionyl-tRNA synthetase. *Nat. Struct. Mol. Biol. 12*, 931–932.
8. Fukai, S., Nureki, O., Sekine, S., Shimada, A., Vassylyev, D. G., and Yokoyama, S. (2003) Mechanism of molecular interactions for tRNA(Val) recognition by valyl-tRNA synthetase. *RNA 9*, 100–111.
9. Klipcan, L., Levin, I., Kessler, N., Moor, N., Finarov, I., and Safro, M. (2008) The tRNA-induced conformational activation of human mitochondrial phenylalanyl-tRNA synthetase. *Structure 16*, 1095–1104.
10. Delagoutte, B., Moras, D., and Cavarelli, J. (2000) tRNA aminoacylation by arginyl-tRNA synthetase: Induced conformations during substrates binding. *EMBO J. 19*, 5599–5610.
11. Sherlin, L. D., and Perona, J. J. (2003) tRNA-dependent active site assembly in a class I aminoacyl-tRNA synthetase. *Structure 11*, 591–603.
12. Schulman, L. H., and Pelka, H. (1988) Anticodon switching changes the identity of methionine and valine transfer RNAs. *Science 242*, 765–768.
13. Martinis, S. A., and Schimmel, P. (1992) Enzymatic aminoacylation of sequence-specific RNA minihelices and hybrid duplexes with methionine. *Proc. Natl. Acad. Sci. U.S.A. 89*, 65–69.
14. Martinis, S. A., and Schimmel, P. (1993) Microhelix aminoacylation by a class I tRNA synthetase. Non-conserved base pairs required for specificity. *J. Biol. Chem. 268*, 6069–6072.
15. Mechulam, Y., Schmitt, E., Maveyraud, L., Zelwer, C., Nureki, O., Yokoyama, S., Konno, M., and Blanquet, S. (1999) Crystal structure of *Escherichia coli* methionyl-tRNA synthetase highlights species-specific features. *J. Mol. Biol. 294*, 1287–1297.
16. Ghosh, G., Pelka, H., and Schulman, L. H. (1990) Identification of the tRNA anticodon recognition site of *Escherichia coli* methionyl-tRNA synthetase. *Biochemistry 29*, 2220–2225.
17. Cassio, D., and Waller, J. P. (1971) Modification of methionyl-tRNA synthetase by proteolytic cleavage and properties of the trypsin-modified enzyme. *Eur. J. Biochem. 20*, 283–300.
18. Alexander, R. W., Nordin, B. E., and Schimmel, P. (1998) Activation of microhelix charging by localized helix destabilization. *Proc. Natl. Acad. Sci. U.S.A. 95*, 12214–12219.
19. Rould, M. A., Perona, J. J., Soll, D., and Steitz, T. A. (1989) Structure of *E. coli* glutaminyl-tRNA synthetase complexed with tRNA(Gln) and ATP at 2.8 Å resolution. *Science 246*, 1135–1142.
20. Sekine, S., Nureki, O., Dubois, D. Y., Bernier, S., Chenevert, R., Lapointe, J., Vassylyev, D. G., and Yokoyama, S. (2003) ATP binding by glutamyl-tRNA synthetase is switched to the productive mode by tRNA binding. *EMBO J. 22*, 676–688.
21. Hauenstein, S., Zhang, C. M., Hou, Y. M., and Perona, J. J. (2004) Shape-selective RNA recognition by cysteinyl-tRNA synthetase. *Nat. Struct. Mol. Biol. 11*, 1134–1141.
22. Fukunaga, R., and Yokoyama, S. (2005) Aminoacylation complex structures of leucyl-tRNA synthetase and tRNA(Leu) reveal two modes of discriminator-base recognition. *Nat. Struct. Mol. Biol. 12*, 915–922.
23. Kim, S., and Schimmel, P. (1992) Functional independence of microhelix aminoacylation from anticodon binding in a class I tRNA synthetase. *J. Biol. Chem. 267*, 15563–15567.
24. Alexander, R. W., and Schimmel, P. (1999) Evidence for breaking domain-domain functional communication in a synthetase-tRNA complex. *Biochemistry 38*, 16359–16365.
25. Budiman, M. E., Knaggs, M. H., Fetrow, J. S., and Alexander, R. W. (2007) Using molecular dynamics simulations to map interaction networks in an aminoacyl-tRNA synthetase. *Proteins: Struct., Funct., Genet. 68*, 670–689.
26. Ghosh, A., and Vishveshwara, S. (2007) A study of communication pathways in methionyl-tRNA synthetase by molecular dynamics simulations and structure network analysis. *Proc. Natl. Acad. Sci. U.S.A. 104*, 15711–15716.
27. Ghosh, A., and Vishveshwara, S. (2008) Variations in clique and community patterns in protein structures during allosteric communication: Investigation of dynamically equilibrated structures of methionyl tRNA synthetase complexes. *Biochemistry 47*, 11398–11407.
28. Anthony, L. C., Dombkowski, A. A., and Burgess, R. R. (2002) Using disulfide bond engineering to study conformational changes in the β-260−309 coiled-coil region of *Escherichia col*i RNA polymerase during σ^{70} binding. *J. Bacteriol. 184*, 2634–2641.
29. Anthony, L. C., and Burgess, R. R. (2002) Conformational flexibility in σ^{70} region 2 during transcription initiation. *J. Biol. Chem. 277*, 46433–46441.
30. Sorenson, M. K., and Darst, S. A. (2006) Disulfide cross-linking indicates that FlgM-bound and free σ28 adopt similar conformations. *Proc. Natl. Acad. Sci. U.S.A. 103*, 16722–16727.
31. Gleghorn, M. L., Davydova, E. K., Rothman-Denes, L. B., and Murakami, K. S. (2008) Structural basis for DNA-hairpin promoter recognition by the bacteriophage N4 virion RNA polymerase. *Mol. Cell 32*, 707–717.
32. Schultz-Heienbrok, R., Maier, T., and Strater, N. (2005) A large hinge bending domain rotation is necessary for the catalytic function of *Escherichia coli* 5′-nucleotidase. *Biochemistry 44*, 2244–2252.
33. Asgeirsson, B., Adalbjornsson, B. V., and Gylfason, G. A. (2007) Engineered disulfide bonds increase active-site local stability and reduce catalytic activity of a cold-adapted alkaline phosphatase. *Biochim. Biophys. Acta 1774*, 679–687.
34. Perona, J. J., Rould, M. A., Steitz, T. A., Risler, J. L., Zelwer, C., and Brunie, S. (1991) Structural similarities in glutaminyl- and methionyl-tRNA synthetases suggest a common overall orientation of tRNA binding. *Proc. Natl. Acad. Sci. U.S.A. 88*, 2903–2907.
35. Ellman, G. L. (1959) Tissue sulfhydryl groups. *Arch. Biochem. Biophys. 82*, 70–77.
36. Sherlin, L. D., Bullock, T. L., Nissan, T. A., Perona, J. J., Lariviere, F. J., Uhlenbeck, O. C., and Scaringe, S. A. (2001) Chemical and enzymatic synthesis of tRNAs for high-throughput crystallization. *RNA 7*, 1671–1678.
37. Landro, J. A., and Schimmel, P. (1993) Metal-binding site in a class I tRNA synthetase localized to a cysteine cluster inserted into nucleotide-binding fold. *Proc. Natl. Acad. Sci. U.S.A. 90*, 2261–2265.
38. Posorske, L. H., Cohn, M., Yanagisawa, N., and Auld, D. S. (1979) Methionyl-tRNA synthetase of *Escherichia coli*. A zinc metalloprotein. *Biochim. Biophys. Acta 576*, 128–133.
39. Crepin, T., Schmitt, E., Mechulam, Y., Sampson, P. B., Vaughan, M. D., Honek, J. F., and Blanquet, S. (2003) Use of analogues of methionine and methionyl adenylate to sample conformational

changes during catalysis in *Escherichia coli* methionyl-tRNA synthetase. *J. Mol. Biol. 332*, 59–72.
40. Calendar, R., and Berg, P. (1966) The catalytic properties of tyrosyl ribonucleic acid synthetases from *Escherichia coli* and *Bacillus subtilis*. *Biochemistry 5*, 1690–1695.
41. Tukalo, M., Yaremchuk, A., Fukunaga, R., Yokoyama, S., and Cusack, S. (2005) The crystal structure of leucyl-tRNA synthetase complexed with tRNALeu in the post-transfer-editing conformation. *Nat. Struct. Mol. Biol. 12*, 923–930.
42. Mascarenhas, A. P., and Martinis, S. A. (2008) Functional segregation of a predicted "hinge" site within the beta-strand linkers of *Escherichia coli* leucyl-tRNA synthetase. *Biochemistry 47*, 4808–4816.
43. Weimer, K. M., Shane, B. L., Brunetto, M., Bhattacharyya, S., and Hati, S. (2009) Evolutionary basis for the coupled-domain motions in *Thermus thermophilus* leucyl-tRNA synthetase. *J. Biol. Chem. 284*, 10088–10099.
44. Yaremchuk, A., Kriklivyi, I., Tukalo, M., and Cusack, S. (2002) Class I tyrosyl-tRNA synthetase has a class II mode of cognate tRNA recognition. *EMBO J. 21*, 3829–3840.
45. Schmitt, E., Meinnel, T., Blanquet, S., and Mechulam, Y. (1994) Methionyl-tRNA synthetase needs an intact and mobile ^{332}KMSKS^{336} motif in catalysis of methionyl adenylate formation. *J. Mol. Biol. 242*, 566–576.
46. Sowdhamini, R., Srinivasan, N., Shoichet, B., Santi, D. V., Ramakrishnan, C., and Balaram, P. (1989) Stereochemical modeling of disulfide bridges. Criteria for introduction into proteins by site-directed mutagenesis. *Protein Eng. 3*, 95–103.
47. Meinnel, T., Mechulam, Y., Le Corre, D., Panvert, M., Blanquet, S., and Fayat, G. (1991) Selection of suppressor methionyl-tRNA synthetases: Mapping the tRNA anticodon binding site. *Proc. Natl. Acad. Sci. U.S.A. 88*, 291–295.
48. Bilokapic, S., Maier, T., Ahel, D., Gruic-Sovulj, I., Soll, D., Weygand-Durasevic, I., and Ban, N. (2006) Structure of the unusual seryl-tRNA synthetase reveals a distinct zinc-dependent mode of substrate recognition. *EMBO J. 25*, 2498–2509.
49. Yadavalli, S. S.; Klipcan, L.; Zozulya, A.; Banerjee, R.; Svergun, D.; Safro, M.; Ibba, M. (2009) *FEBS Letters* , in press.